Supporting Information for:

Fano Resonance and Incoherent Interlayer Excitons in Molecular van der Waals Heterostructures

Carlos R. Lien-Medrano,[1] Franco P. Bonafé,[2] Chi Yung Yam,[3] Carlos-Andres Palma,[*,4,5] Cristián G. Sanchez[*,6] and Thomas Frauenheim[7,3,1]

[1]Bremen Center for Computational Materials Science, University of Bremen, Bremen 28359, Germany

[2]Max Planck Institute for the Structure and Dynamics of Matter, Hamburg 22761, Germany

[3]Shenzen JL Computational Science and Applied Research Institute (CSAR), Shenzhen 518110, P. R. China

[4]Institute of Physics, Chinese Academy of Sciences, Beijing 100190, P.R. China

[5]Department of Physics & IRIS Adlershof, Humboldt-Universität zur Berlin, Berlin 12489, Germany

[6]Instituto Interdisciplinario de Ciencias Básicas, Universidad Nacional de Cuyo, Mendoza M5502JMA, Argentina

[7] Beijing Computational Science Research Center, 100193 Beijing, P.R. China

[*] E-mail: palma@iphy.ac.cn, csanchez@mendoza-conicet.gob.ar

1 Computational methods

1.1 Real time time-dependent density tigth-binding

We have used the DFTB+ package (*1*), an implementation of the DFTB method, to obtain the GS Hamiltonian (H_{GS}) and overlap matrix (S). Using the H_{GS} and the S matrix, we computed the the initial GS reduced single-electron density matrix (ρ). The mio-1-1 DFTB parameters set was employed to obtain the electronic structure of all the structures presented in this work. In order to describe the electronic dynamics of the systems under study we need to extend the DFTB method to the time-domain (TD-DFTB). On the basis of a real-time propagation of ρ under the influence of a time-varying external field, we can obtain excited-state properties of the systems. This propagation is achieved through the numerical integration of the Liouville-von Neumann equation of motion in the non-orthogonal basis:

$$\dot{\rho} = -\mathrm{i}(S^{-1}H\rho - \rho H S^{-1}).$$

For more details on the theoretical method and its computational implementation, please refer to Bonafé et al. (*2*). By applying a perturbation in the shape of a Dirac delta to the Hamiltonian, within the linear response regime, we can obtain the absorption spectra of the sytems as follows. The dipole moment is given by:

$$\boldsymbol{\mu}(t) = \int_0^\infty \boldsymbol{\alpha}(t-\tau)E(\tau)d\tau,$$

where $\boldsymbol{\alpha}(t-\tau)$ is the polarizability along the axis over which the external field $\mathbf{E}(\tau)$ is applied. After the deconvolution of the applied electric field, the frequency

dependent polarizability α can be obtained:

$$\boldsymbol{\alpha}(\omega) = \frac{\boldsymbol{\mu}(\omega)}{E(\omega)}$$

The imaginary part of the polarizability is proportional to the Absorption spectrum.

For the study of the charge transfer processes, electron dynamics were triggered by the application of a continuous laser-type (sinusoidal) perturbation in tune with the excitation energy of interest.

1.2 Derivation of the adapted Gersten-Nitzan model

Let A and B be two coupled point-dipoles, as depicted in Figure 3 (a) of the main manuscript. They are separated in the x direction by a distance R_{AB}. Both systems are coupled to an external time-dependent electric field $\vec{E}_{\text{ext}}(t)$, which can have any polarization direction within the (x, y) plane. Moreover, both systems are affected by the dipolar electric field generated by the other system. In other words, being $\vec{E}_A$ and $\vec{E}_B$ the effective electric fields acting on both systems,

$$\vec{E}_A(t) = \vec{E}_{\text{ext}}(t) + \vec{E}_{BA}(\vec{R}_A, t)$$
$$\vec{E}_B(t) = \vec{E}_{\text{ext}}(t) + \vec{E}_{AB}(\vec{R}_B, t)$$

where $\vec{E}_{BA}$ and $\vec{E}_{AB}$ are the electric field generated by B acting on A, and the one generated by A acting on B, respectively, defined as:

$$\vec{E}_{BA}(R_A, t) = \int_{-\infty}^{t} \tilde{\chi}_B(\vec{R}_A, t, t')\vec{E}_{\text{ext}}(t')dt' \tag{1}$$
$$\vec{E}_{AB}(R_B, t) = \int_{-\infty}^{t} \tilde{\chi}_A(\vec{R}_B, t, t')\vec{E}_{\text{ext}}(t')dt' \tag{2}$$

Here, $\tilde{\chi}$ is a **dipole-field response function** that is such that when multiplied by the external field and integrated yields the local dipole electric field generated by the system. It has a connection with the dipole susceptibility, which will be explored below. We start with the formula for the electric field of a perfect dipole, and being $\vec{\mu}_I$ be the dipole moment of system I:

$$\vec{E}_{BA} = \frac{1}{4\pi\epsilon_0}\frac{3(\vec{\mu}_B \cdot \hat{R}_{BA})\hat{R}_{BA} - \vec{\mu}_B}{R^3_{BA}} \tag{3}$$

As usual, $\vec{R}_{BA} = \vec{R}_A - \vec{R}_B$. By construction of the model, $\vec{R}_{BA} = -R_{AB}\hat{x}$, which means $\hat{R}_{BA} = -\hat{x}$; and $\vec{R}_{AB} = R_{AB}\hat{x}$, ergo $\hat{R}_{AB} = \hat{x}$. By inserting the position vectors into eq. 3, we get:

$$\vec{E}_{BA} = \frac{1}{4\pi\epsilon_0}\frac{2\mu_{B_x}\hat{x} - \mu_{B_y}\hat{y}}{R^3_{AB}} \tag{4}$$

Now, by definition of the dipole response function χ, and neglecting image field effects,

$$\vec{\mu}_B(t) = \vec{\mu}^0_B + \int_{-\infty}^{t} \chi^B(t,t')\vec{E}_{\text{ext}}(t')dt' \tag{5}$$

Inserting 5 into 4:

$$\vec{E}_{BA} = \int_{-\infty}^{t} \frac{1}{4\pi\epsilon_0 R^3_{AB}} \begin{pmatrix} 2 & 0 \\ 0 & -1 \end{pmatrix} \cdot \chi^B(t,t') \cdot \vec{E}_{\text{ext}}(t')dt' \tag{6}$$

which by comparison with 1, allows us to define $\tilde{\chi}$ for system B:

$$\tilde{\chi}_B = \frac{1}{4\pi\epsilon_0 R^3_{AB}} \begin{pmatrix} 2 & 0 \\ 0 & -1 \end{pmatrix} \chi^B(t,t') \tag{7}$$

As everything is symmetric under the exchange of labels $A \to B$ and $B \to A$, we get now for $\vec{E}_{AB}$ and $\tilde{\chi}_A$ the following:

$$\vec{E}_{AB} = \int_{-\infty}^{t} \frac{1}{4\pi\epsilon_0 R_{AB}^3} \begin{pmatrix} 2 & 0 \\ 0 & -1 \end{pmatrix} \chi^A(t,t') \cdot \vec{E}_{\text{ext}}(t'))dt' \tag{8}$$

$$\tilde{\chi}_A = \frac{1}{4\pi\epsilon_0 R_{AB}^3} \begin{pmatrix} 2 & 0 \\ 0 & -1 \end{pmatrix} \chi^A(t,t') \tag{9}$$

Our goal is to get the polarizability of the combined system under the effect of the external field and of the dipolar field induced in the neighbour system, using as inputs the polarizabilities of the isolated systems. Then, we need to calculate both terms of the total dipole $\vec{\mu}(t) = \vec{\mu}_A(t) + \vec{\mu}_B(t)$. Starting with $\vec{\mu}_A(t)$, we have the the external field and the induced dipolar field terms:

$$\vec{\mu}_A(t) = \int_{-\infty}^{t} dt' \chi^A(t,t') \vec{E}_{\text{ext}}(t') + \int_{-\infty}^{t} \int_{-\infty}^{t'} dt' dt'' \chi^A(t,t') D \chi^B(t',t'') \vec{E}_{\text{ext}}(t'') \tag{10}$$

where $D := \frac{1}{4\pi\epsilon_0 R_{AB}^3} \begin{pmatrix} 2 & 0 \\ 0 & -1 \end{pmatrix}$ is the geometrical factor. Calculating the Fourier transform of 10:

$$\vec{\mu}_A(\omega) = [\alpha^A(\omega) + \alpha^A(\omega) D \alpha^B(\omega)] \vec{E}(\omega) \tag{11}$$

And equivalently for B:

$$\vec{\mu}_B(\omega) = [\alpha^B(\omega) + \alpha^B(\omega) D \alpha^A(\omega)] \vec{E}(\omega) \tag{12}$$

These expressions suggest a natural definition of an effective polarizability, which can be written as:

$$\alpha^{\text{eff},A} = \alpha^{A}(\omega) + \alpha^{A}(\omega) D\alpha^{B}(\omega) \tag{13}$$

$$\alpha^{\text{eff},B} = \alpha^{B}(\omega) + \alpha^{B}(\omega) D\alpha^{A}(\omega) \tag{14}$$

Which is the formula used to calculate the polarizability components shown in Figure 3 of the main manuscript.

2 Figs. S1 to S6

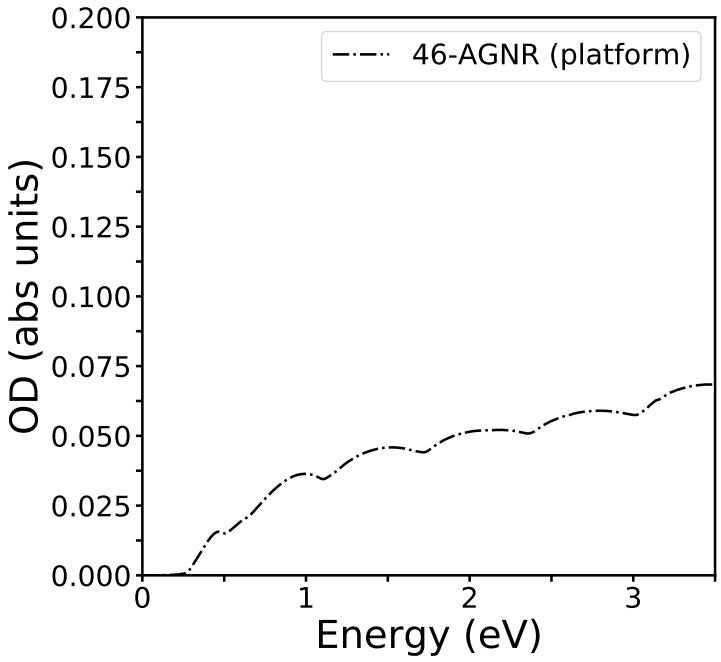

Fig. S1. Absorption spectrum of 46-AGNR.

The figure shows the absorption spectrum of the 46 atom width Armchair graphene nanoribbon (46-AGNR) used as the platform in the van der Waals molecular heterostructure presented in this work.

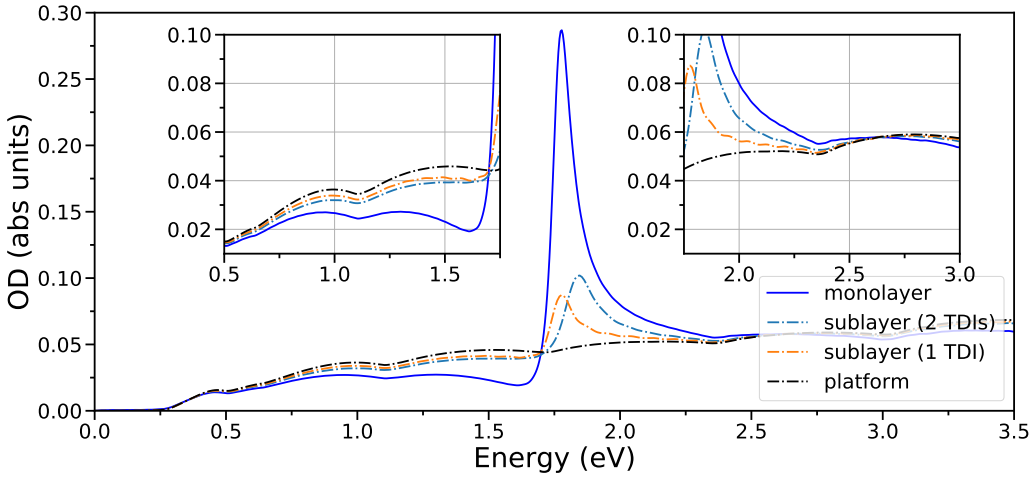

Fig. S2 Coverage absorption dependency. Absorption spectrum of different sublayers of TDI molecules on top of the ribbon platform. As a reference, in blue is plotted the same monolayer spectrum as in the manuscript (6 TDI molecules in the unit cell).

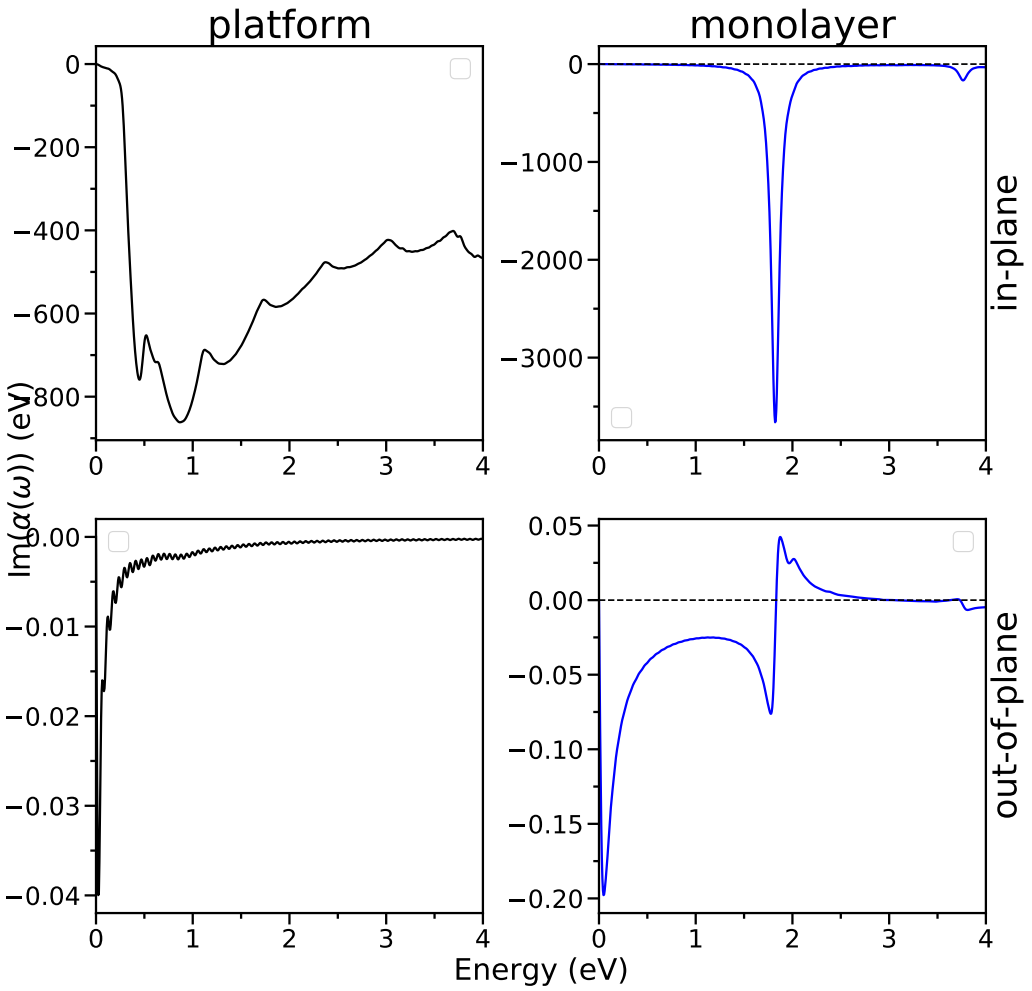

Fig. S3. Individual polarizabilities for system 1a. (**A**) In-plane and out-of-plane polarizabilities for the platform. (**B**) In-plane and out-of-plane polarizabilities for the monolayer of TDI.

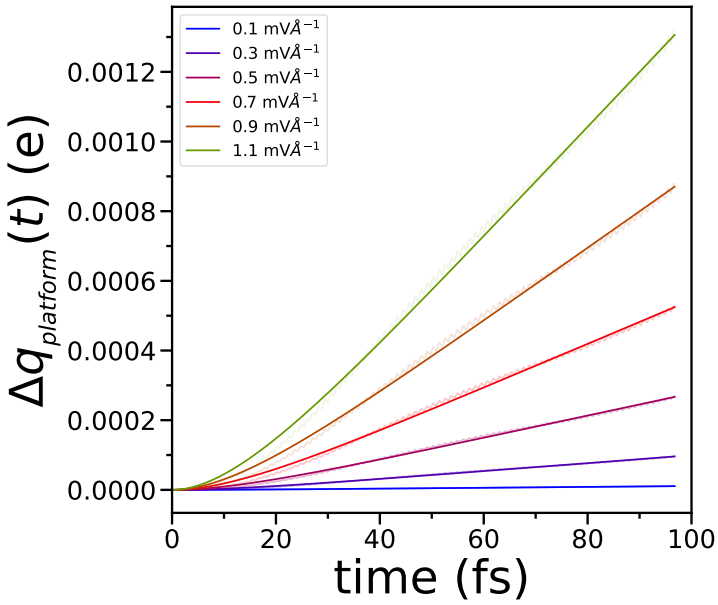

Fig. S4. Charge transfer $\Delta q(t)$ of the platform for different field strengths as obtained from the dynamical simulations.

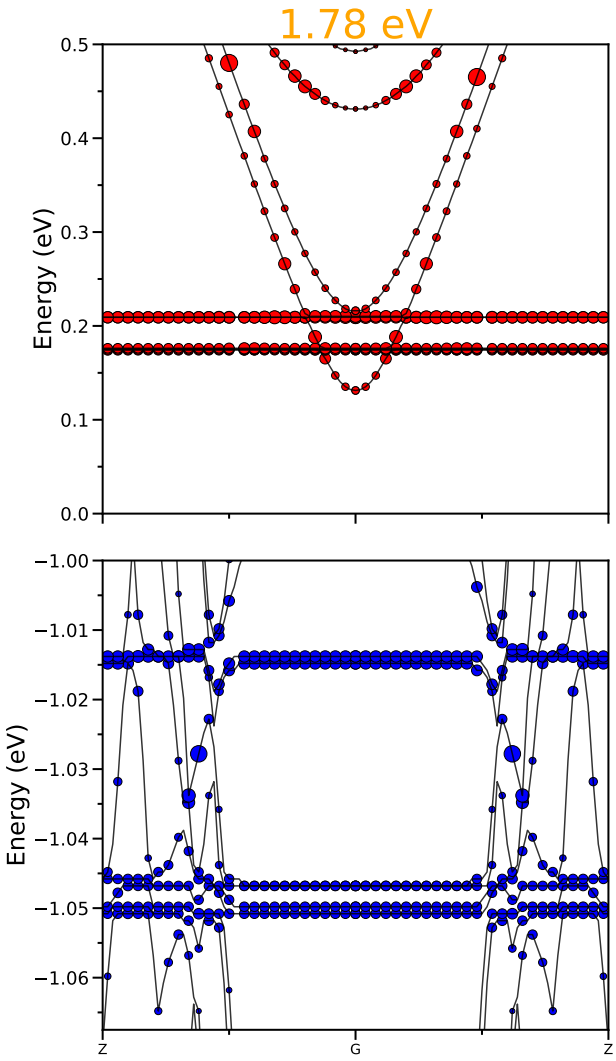

Fig. S5. Detail of Fig. 2c showing the band structure and populations for excitation at 1.78 in the energy regions corresponding to the HOMO and LUMO orbitals of the monolayer. Red (blue) circles denote the increase (decrease) of electron occupation and the circle size is proportional to the change of population.

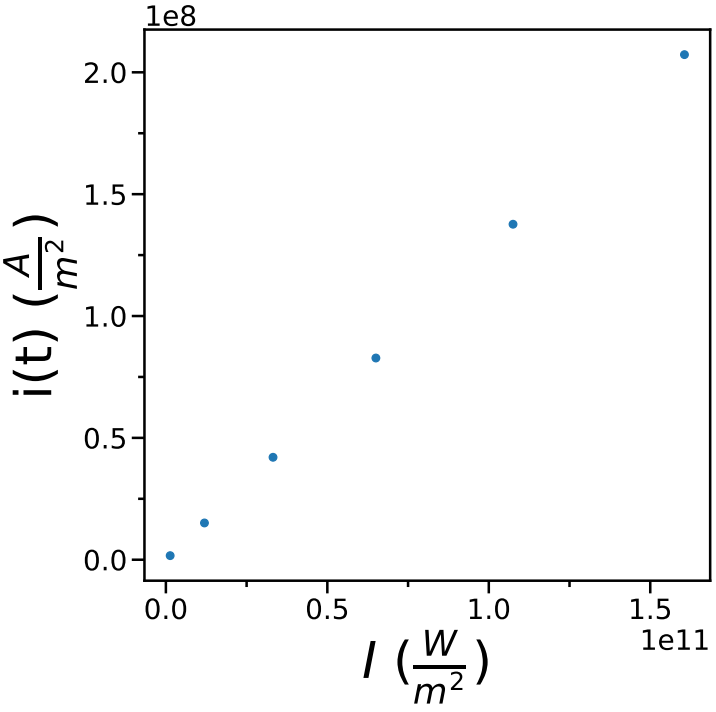

Fig. S6. Photoresponse shown as interlayer current as a function of laser intensity. Currents where obtained from the stationary state (linear) portion of the time dependent charge shown in Figure S4.

References

1. B. Hourahine et al. DFTB+, a software package for efficient approximate density functional theory based atomistic simulations. *The Journal of Chemical Physics*, 152(12):124101, 2020.

2. Franco P. Bonafé, Bálint Aradi, Ben Hourahine, Carlos R. Medrano, Federico J. Hernández, Thomas Frauenheim, and Cristián G. Sánchez. A Real-Time Time-Dependent Density Functional Tight-Binding Implementation for Semiclassical Excited State Electron–Nuclear Dynamics and Pump–Probe Spectroscopy Simulations. *Journal of Chemical Theory and Computation*, 16(7):4454–4469, 2020.